



Molecular Dissection of VirB, a Key Regulator of the Virulence Cascade of *Shigella flexneri*

Christophe Beloin, Sorchia Mckenna, Charles J. Dorman

► To cite this version:

Christophe Beloin, Sorchia Mckenna, Charles J. Dorman. Molecular Dissection of VirB, a Key Regulator of the Virulence Cascade of *Shigella flexneri*. *Journal of Biological Chemistry*, 2002, 277 (18), pp.15333-15344. 10.1074/jbc.M111429200 . hal-03217821

HAL Id: hal-03217821

<https://hal.science/hal-03217821>

Submitted on 5 May 2021

HAL is a multi-disciplinary open access archive for the deposit and dissemination of scientific research documents, whether they are published or not. The documents may come from teaching and research institutions in France or abroad, or from public or private research centers.

L'archive ouverte pluridisciplinaire **HAL**, est destinée au dépôt et à la diffusion de documents scientifiques de niveau recherche, publiés ou non, émanant des établissements d'enseignement et de recherche français ou étrangers, des laboratoires publics ou privés.



Distributed under a Creative Commons Attribution 4.0 International License

Molecular Dissection of VirB, a Key Regulator of the Virulence Cascade of *Shigella flexneri**

Received for publication, November 30, 2001, and in revised form February 8, 2002
Published, JBC Papers in Press, February 15, 2002, DOI 10.1074/jbc.M111429200

Christophe Beloin‡, Sorcha McKenna, and Charles J. Dorman§

From the Department of Microbiology, Moyne Institute of Preventive Medicine, Trinity College Dublin, Dublin 2, Republic of Ireland

The VirB protein is a key regulator of virulence gene expression in the facultative enteroinvasive pathogen *Shigella flexneri*. While genetic evidence has shown that it is required for activation of transcription of virulence genes located on a 230-kb plasmid in this bacterium, hitherto, evidence that VirB is a DNA-binding protein has been lacking. Although VirB shows extensive homology to proteins involved in plasmid partitioning, it does not resemble any known conventional transcription factor. Here we show for the first time that VirB binds to the promoter regions of the virulence genes *in vivo*. We also show that VirB forms dimeric and higher oligomeric structures both *in vivo* and *in vitro* and that this property is independent of DNA binding. The oligomerization activity of VirB is distributed over two domains: a leucine zipper-like motif and a carboxyl-terminal domain likely to form triple coiled structures. VirB possesses a helix-turn-helix motif, which is required for DNA binding. The amino-terminal domain of the protein is also required for DNA binding and virulence gene activation. The possibility that VirB requires a co-factor for specific interaction with target promoters *in vivo* is discussed.

Shigella flexneri is a Gram-negative, facultative intracellular pathogen of humans and primates and is the causative agent of bacillary dysentery. This extremely infectious disease is widespread in the developing world, where it is responsible for around 600,000 deaths per annum, most particularly affecting children (1).

The gene products that mediate the invasion of the lower intestine by *Shigella* are located on a 230-kb large virulence plasmid, where they are clustered in a 31-kb segment called the entry region. Here are found the *ipa* genes, which encode secreted invasins responsible for macrophage apoptosis, epithelial cell invasion, and vesicle escape (2–4); the *mxi* and *spa* genes, encoding the type III secretion system for export of the *ipa* gene products (5); and the *icsA*, *icsB*, and *virA* genes required for cell-to-cell spread (5, 6). It is likely that expression of these structural genes represents a large metabolic burden for the bacteria. Therefore, it is unsurprising that the bacterium has evolved a complex regulatory system that integrates sev-

eral environmental signals to prevent inappropriate expression. At the transcriptional level, a cascade that involves both chromosomally encoded proteins including IHF (integration host factor) and H-NS (histone-like nucleoid structuring protein) and plasmid-encoded regulatory proteins, VirF and VirB, restricts expression of the structural genes to conditions that approximate those in the lower intestine (*i.e.* a pH optimum of 7.4, moderate osmolarity, and a temperature of 37 °C (see Refs. 7–10; for a review, see Ref. 11)).

VirF is an AraC-like transcription factor responsible for activation of regulatory gene *virB* and structural gene *icsA* and autorepression of *virF* (12–14). The *virB* gene product in turn activates expression of the remaining structural genes required for virulence via an unknown mechanism. VirB expression is also regulated by H-NS, which, together with levels of negative DNA supercoiling, appears to be responsible for the temperature dependence of *virB* transcription (8, 10, 15). Sensitivity to levels of negative DNA supercoiling also appears to be responsible for the osmoregulation of *virB* expression (8, 15). Recently, *virB* expression was shown to be regulated by quorum sensing (16).

The VirB protein was first identified through transposon mutagenesis of the virulence plasmid (17), when it was shown to be essential for the expression of almost all of the structural virulence genes. VirB possesses no homology to previously described conventional transcriptional activators. Small and basic, VirB (35.4 kDa) shows most homology at the amino acid sequence level to ParB and SopB, proteins that are involved in plasmid partition and the maintenance of stable plasmid copy number, on the P1/P7 and F plasmids, respectively (17–21). This homology is most pronounced in the first two-thirds of the proteins that includes, in ParB, a helix-turn-helix (HTH)¹ motif (22), whereas the C-terminal parts, encompassing in ParB its major oligomerization domain, are more divergent (20, 23). The domain structure and activity of the VirB protein are unknown, and it has been assumed that VirB is in some way acting as a conventional transcriptional activator at the promoters of the structural virulence genes. Thus far, evidence that VirB activates structural gene expression directly is lacking, as is evidence that it is a DNA-binding protein.

The aim of this work is to identify the important structural domains within the VirB protein and to understand how this unusual protein regulates virulence gene expression in *S. flexneri*. Extensive mutational and deletion analyses were carried out. VirB derivatives harboring point mutations or truncations were analyzed for their ability to activate gene expression and to bind DNA and for their *trans*-dominant phenotype, and they

* This work was supported by European Union Training and Mobility of Researchers Award ERBFMRXCT98-0164 and Enterprise Ireland Grant SC/99/432. The costs of publication of this article were defrayed in part by the payment of page charges. This article must therefore be hereby marked "advertisement" in accordance with 18 U.S.C. Section 1734 solely to indicate this fact.

‡ Present address: Groupe de Génétique des Biofilms, Institut Pasteur, 25 rue du Dr. Roux, 75724 Paris, Cedex 15, France.

§ To whom correspondence should be addressed. Tel.: 353-1-608-2013; Fax: 353-1-679-9294; E-mail: cjdorman@tcd.ie.

¹ The abbreviations used are: HTH, helix-turn-helix; Cm, chloramphenicol; Ca, carbenicillin; Tet, tetracycline; Km, kanamycin; PBS, phosphate-buffered saline; DSP, dithiobis(succinimidyl propionate); LVP, large virulence plasmid; LZ, leucine zipper.

TABLE I
Bacterial strains, plasmids, and phage

Strain or plasmid	Relevant characteristics	Source/Reference
Strains		
<i>S. flexneri</i>		
BS184	<i>mxiC</i> ::MudI1734, Km ^r	Ref. 39
CJD1018	BS184 <i>virB</i> ::Ap, Ca ^r Km ^r	Ref. 9
<i>E. coli</i>		
XL-1 Blue	<i>supE44hsdR17recA1endA1gyrA46thi relA1lac⁻ F[proAB⁺ lacI^a lacZΔM15Tn10], Tet^r</i>	Stratagene
DH5α	<i>supE44 ΔlacU169(φ80 lacZΔM15) hsdR17recA1endA1gyrA96thi-1relA1</i>	Ref. 51
AG1688	<i>hsdRmcrBaraD139Δ(araABC-leu)7679ΔlacX7 4galUgalKrrsLthiF' 128lacIqlacZ::Tn5, Km^r</i>	<i>E. coli</i> GCG
JH372	AG1688(λ)202, Km ^r	Ref. 26
JH607	AG1688 (λ)1120 _{P_s} , Km ^r	Ref. 26
BL21DE3	<i>hsdSgal (ΔcIts857ind1Sam7nin5lacUV5-T7gene1)</i>	Ref. 52
Plasmids		
pBC	Cloning vector; ColE1 replicon, Cm ^r	Stratagene
pACYC184	Cloning vector; p15A replicon, Cm ^r Tet ^r	Stratagene
pET22b	His tag expression vector, Ca ^r	Novagen
pBCP378	Expression vector; ColE1 replicon, Ca ^r	Ref. 53
pMEP539	<i>cat</i> gene in pBCP378, Ca ^r Cm ^r	Ref. 9
pMEP538	<i>virB</i> gene in pMEP539, Ca ^r Cm ^r	Ref. 9
pBCPK152E	pMEP538 with K152E mutation, Ca ^r Cm ^r	This work
pBCPK164E	pMEP538 with K164E mutation, Ca ^r Cm ^r	This work
pBCPL196E	pMEP538 with L196E mutation, Ca ^r Cm ^r	This work
pBCPL203P	pMEP538 with L203P mutation, Ca ^r Cm ^r	This work
pBCPL203V	pMEP538 with L203V mutation, Ca ^r Cm ^r	This work
pBCPN207H	pMEP538 with N207H mutation, Ca ^r Cm ^r	This work
pBCPN207I	pMEP538 with N207I mutation, Ca ^r Cm ^r	This work
pBCPL210H	pMEP538 with L210H mutation, Ca ^r Cm ^r	This work
pBCPL210P	pMEP538 with L210P mutation, Ca ^r Cm ^r	This work
pBCPP215A	pMEP538 with P215A mutation, Ca ^r Cm ^r	This work
pBCPL217S	pMEP538 with L217S mutation, Ca ^r Cm ^r	This work
pBCPL224R	pMEP538 with L224R mutation, Ca ^r Cm ^r	This work
pBCPK152E L203P	pMEP538 with K152E + L203P, Ca ^r Cm ^r	This work
pBCPK152E L210P	pMEP538 with K152E + L210P, Ca ^r Cm ^r	This work
pBCPΔ1–30	pMEP538 with Δ1–30 deletion, Ca ^r Cm ^r	This work
pBCPΔ1–65	pMEP538 with Δ1–65 deletion, Ca ^r Cm ^r	This work
pBCPΔ244–309	pMEP538 with Δ244–309 deletion, Ca ^r Cm ^r	This work
pBCPΔ262–309	pMEP538 with Δ262–309 deletion, Ca ^r Cm ^r	This work
pBCPΔ292–309	pMEP538 with Δ292–309 deletion, Ca ^r Cm ^r	This work
pBCPΔLZ	pMEP538 with ΔLZ deletion, Ca ^r Cm ^r	This work
pJH391	“Stuffer” plasmid: pJH370, with <i>SalI</i> - <i>SacI</i> <i>lacZ</i> fragment from pMC1871, deletion between <i>Bam</i> HI, Ca ^r	Ref. 26
pFG157	pZ150 with intact λ cI repressor, Ca ^r	Ref. 26
pZ150	pBR322 with M13 ssDNA <i>ori</i> , Ca ^r	Ref. 54
pJH370	pFG157 1–115 of λ cI + GCN4 LZ on <i>Hind</i> III- <i>Eco</i> RV fragment, Ca ^r	Ref. 26
pKH101	pFG157 Δ115–237 λ cI repressor, Ca ^r Cm ^r	Ref. 26
pMC1871	Multipurpose cloning vector, Ca ^r	Ref. 55
pSMvirB	pJH391 with <i>virB</i> fused to λ cI1–115, Ca ^r	This work
pSML203P	pSMvirB with L203P mutation, Ca ^r	This work
pSMK152E	pSMvirB with K152E mutation, Ca ^r	This work
pSMΔ1–144	pSMvirB with Δ1–144 deletion, Ca ^r	This work
pSMΔ1–184	pSMvirB with Δ1–184 deletion, Ca ^r	This work
pSMΔ1–225	pSMvirB with Δ1–225 deletion, Ca ^r	This work
pSMΔ232–309	pSMvirB with Δ232–309 deletion, Ca ^r	This work
pSMΔ176–309	pSMvirB with Δ176–309 deletion, Ca ^r	This work
pSMΔ147–309	pSMvirB with Δ147–309 deletion, Ca ^r	This work
pSMHTH	pSMvirB with VirB HTH, Ca ^r	This work
pSMLZ	pSMvirB with VirB LZ, Ca ^r	This work
Phage		
λ vir	KH54 h80	Ref. 26
λ cI ⁻	KH54 ΔcI ⁻	Ref. 26

were also used in *in vivo* cross-linking analysis to determine their ability to oligomerize. Here we present evidence that VirB possesses separate structural domains responsible for its oligomerization, DNA binding, and transcription activation properties. Moreover, evidence is presented that VirB is able to bind *in vivo* to the promoter regions of the structural virulence genes, supporting the hypothesis that VirB activates these genes directly.

EXPERIMENTAL PROCEDURES

Bacterial Strains, Plasmids, and Growth Conditions

The bacterial strains and plasmids used are listed in Table I. Antibiotics used in selective media were chloramphenicol (Cm; 20 μg/ml),

carbenicillin (Ca; 50 μg/ml), tetracycline (Tet; 10 μg/ml), and kanamycin (Km; 50 μg/ml). Cells were grown in Luria Broth (LB). LB agar plates supplemented with 5-bromo-4-chloro-3-indolyl-β-D-galactopyranoside (X-gal) at a concentration of 40 μg/ml, and MacConkey Lactose agar plates were used to indicate levels of β-galactosidase activity.

Site-directed Mutagenesis and Truncation of VirB

The *virB* gene previously cloned in pMEP538 (9) was sequenced to confirm its integrity. This plasmid is derived from pMEP539 (9), a derivative of expression vector pBC378 that contains a *cat* gene (Table I). Derivatives of pMEP538 with mutations in the *virB* gene were constructed using the Stratagene QuikChange[®] kit. Each mutant was sequenced to confirm the presence of the mutation. Truncates of VirB were constructed by amplifying truncated forms of the *virB* gene by

PCR and cloning into the *Nde*I and *Sal*I restriction sites of pMEP539. The leucine zipper (LZ) motif deletion truncate was constructed by three-way cloning into the same sites. Putative clones of each truncate were sequenced, and expression of truncates was confirmed by western immunoblotting.

Bioinformatic Analysis of VirB Tertiary Structure

The program HTH (24) was used for detection of a possible HTH DNA-binding motif in VirB. The programs COILS, MULTICOIL, and PARCOIL from the Expasy Web server (www.expasy.ch/) were used to analyze the tertiary structure of the LZ motif and the C terminus of VirB.

β -Galactosidase Assays

Transcription of the *mxiC-lacZ* fusion was monitored by β -galactosidase assay of cells cultured overnight, according to Miller (25). Assays were performed at least in triplicate, and the data are expressed as the mean of two measurements.

Purification of VirB

N-terminal His-tagged VirB was overexpressed in BL21DE3 cells from the pET22b Novagen vector. Expression was induced in exponentially growing 500-ml cultures with 0.1 mM isopropyl-1-thio- β -D-galactopyranoside. After 3 h, the cells were harvested, and lysates were prepared by repeated passage through a French pressure cell. The lysate (~15 ml) was applied to a His-bind® Quick column (Novagen), which had been preequilibrated with binding buffer. The column was then washed with binding buffer (50 ml) and wash buffer (25 ml). The protein was then eluted in 1-ml fractions of 2×15 ml of elution buffer (10% glycerol, 50 mM Tris-HCl, pH 7.9, 0.5 M NaCl, 0.1 mM phenylmethylsulfonyl fluoride) containing 100 or 500 mM imidazole. Fractions were analyzed by SDS-PAGE, and those containing VirB were pooled and dialyzed three times against 1 liter of 50 mM Tris-HCl, pH 7.5, 1 mM EDTA, pH 8, 300 mM NaCl, 5% glycerol, 0.1 mM phenylmethylsulfonyl fluoride, 1 mM dithiothreitol. VirB was estimated to be ~95% pure. Rabbit polyclonal antibodies were conventionally prepared using purified VirB. Prior to immunodetection, the serum was adsorbed against a crude protein extract of a *virB*⁻ *S. flexneri* strain.

Immunodetection of VirB

Total protein extracts were separated through 12% SDS-PAGE. The separated proteins were electroblotted onto a nitrocellulose membrane using the Bio-Rad miniprotein II system for 1 h at 80 V. Nitrocellulose membranes were stained with Ponceau (0.2% Ponceau dye, 3% trichloroacetic acid) to check the efficiency of transfer before being blocked overnight with 5% dried skimmed milk in phosphate-buffered saline (PBS). Detection of VirB was performed in PBS containing 1% dried skimmed milk with a primary polyclonal anti-VirB antiserum (1:500) and a secondary goat anti-rabbit horseradish peroxidase-conjugated antiserum (1:10,000). Membranes were developed using the chemiluminescent Pierce West Pico Super Signal kit.

In Vivo and in Vitro Protein-Protein Cross-linking

In Vivo—Cells were grown overnight at 37 °C in 3 ml of LB medium and diluted to A_{600} 0.05 in 50 ml of LB medium. At A_{600} 0.6, 1 ml of cells were transferred to a microcentrifuge tube and incubated at 37 °C for 30 min with 50 mM iodoacetamide, with or without 25 mM dithiobis(succinimidyl propionate) (DSP). The reaction was quenched by adding 100 mM Tris-HCl, pH 7. A_{600} of the sample was monitored, and the equivalent of 1 ml of A_{600} 0.5 was harvested, washed twice in PBS, and resuspended in 20 μ l of buffer containing 50 mM Tris-HCl, pH 7, 1 mM EDTA, pH 8, 10% glycerol, 200 mM NaCl, 1 mM phenylmethylsulfonyl fluoride (added fresh). 10 μ l of 3 \times Laemmli buffer (without dithiothreitol or 2- β -mercaptoethanol) was added, and samples were boiled for 3 min at 100 °C. Prior to loading, samples were treated during 20 min at 37 °C with 20 units of benzonase. Cross-linked proteins were then separated on a 12% SDS-PAGE. VirB was then immunodetected.

In Vitro—Purified VirB was treated in 100- μ l reaction mixes consisting of 50 ng of protein and 50 mM iodoacetamide in PBS. At time 0, 10 μ l of a 0.1 mM DSP solution in Me_2SO was added. The control tube received an equal volume of Me_2SO alone. The reactions were incubated at 37 °C. 10- μ l samples were removed at fixed time intervals and quenched by the addition of 20 μ l of 3 \times Laemmli buffer followed by boiling for 10 min. Samples were electrophoresed on a 12% SDS-PAGE, and VirB was then detected by Western blotting.

In Vivo Oligomerization Assay

In order to determine the oligomerization properties of VirB and parts of VirB, fusion proteins were constructed by cloning the appropriate fragment of VirB into the *Sal*I–*Bam*HI site in pJH391, thereby creating an in-phase translational fusion to the N terminus (DNA-binding region) of λ cI (see Fig. 6). Each construction was sequenced to verify its integrity. To assess the ability of cloned fragments to oligomerize, two assays were carried out, a phage sensitivity assay and β -galactosidase repression assay (25, 26). Plasmids expressing the chimeric proteins were transformed into *Escherichia coli* strain AG1688, and the strains were infected with λ cI⁻. Strains immune to this phage, as judged by no plaque formation, possess a fragment capable of dimerization fused to the N terminus of cI. Similarly, plasmids were transformed into the strain JH372, and β -galactosidase assays were performed as described above; in this case, a repression of β -galactosidase activity indicated a dimerizing fragment.

Formaldehyde Cross-linking and Immunoprecipitations

Cells were grown in conditions of VirB induction (*i.e.* in LB medium at 37 °C, up to A_{600} ~0.6). Cross-linking and sample preparation were based on chromatin immunoprecipitation assays (27, 28). 10 ml of cells was then transferred to a new vial, and samples were treated with formaldehyde (final concentration 0.1%) for 30 min at 37 °C with shaking. Cells were pelleted, washed twice with PBS, resuspended in 0.5 ml of lysis buffer (10 mM Tris-HCl, pH 8, 20% sucrose, 50 mM NaCl, 10 mM EDTA, pH 8) containing 2 mg/ml of lysozyme and incubated during 30 min at 37 °C. After freeze-thawing, 0.5 ml of 2 \times immunoprecipitation buffer (100 mM Tris-HCl, pH 7, 300 mM NaCl, 2% Triton X-100, 0.2% deoxycholic acid) and phenylmethylsulfonyl fluoride (final concentration 1 mM) was added to the samples, and the cell extract was incubated an additional 10 min at 37 °C. The DNA was then sheared by sonication using a Ca MSE Soniprep 150 sonicator (Sanyo). Insoluble cell debris was removed by centrifugation, and the supernatant was transferred to a new microcentrifuge tube. Protein and protein-DNA complexes were immunoprecipitated with adsorbed polyclonal anti-VirB antibodies (1 h at room temperature on a rotating wheel) followed by incubation with 30 μ l of a 50% protein A-Sepharose slurry (1 h at room temperature with mixing). Complexes were collected by centrifugation and washed five times with 1 ml of 1 \times immunoprecipitation buffer and twice with 1 ml of 1 \times TE (10 mM Tris-HCl, pH 8, 0.1 mM EDTA, pH 8). The slurry was then resuspended in 50 μ l of 1 \times TE. Formaldehyde cross-links were reversed by incubation at 65 °C for 6 h. PCR was performed with *Taq* DNA polymerase using 2 μ l of the immunoprecipitated DNA and a constant amount of either purified *S. flexneri* chromosomal or large virulence plasmid (LVP) DNA as controls. PCRs were carried out with a master-mix containing the primers. The only difference between the samples was the DNA added. All assays were performed several times, and reproducible results were obtained. The identities of the PCR products generated by these primers were confirmed previously by DNA sequencing. Primers were ~25 bp in length and amplified ~300–400-bp products. Sequences of all primers are available upon request. Relative affinities of VirB to different sites were determined by comparing the intensity of bands from the immunoprecipitate and the chromosomal/LVP DNA.

RESULTS

Prediction of Structural Domains in the VirB Protein—As a first approach to identify structural domains of the VirB protein, we analyzed its predicted secondary structure *in silico*. Since VirB is regarded as a putative transcriptional regulator, it was first scanned for the presence of a putative DNA-binding motif. The program HTH (24) predicted at 100% probability the region 148–171 of VirB to contain a typical HTH DNA-binding motif (Fig. 1A) as observed in different prokaryotic transcriptional regulators such as λ Cro, LacR, or CRP (29). The HTH motif consists of two helices separated by a short extended chain of amino acids, which are held at fixed angles by electrostatic interactions between side chains on each helix. The second helix, known as the recognition helix, fits into the major groove of DNA to participate in sequence specific interactions. The first helix, known as the positioning helix, stabilizes this complex by interacting nonspecifically with the DNA backbone. As eukaryotic and prokaryotic HTH DNA-binding motifs are known to interact with their targets as dimers, we also tried to

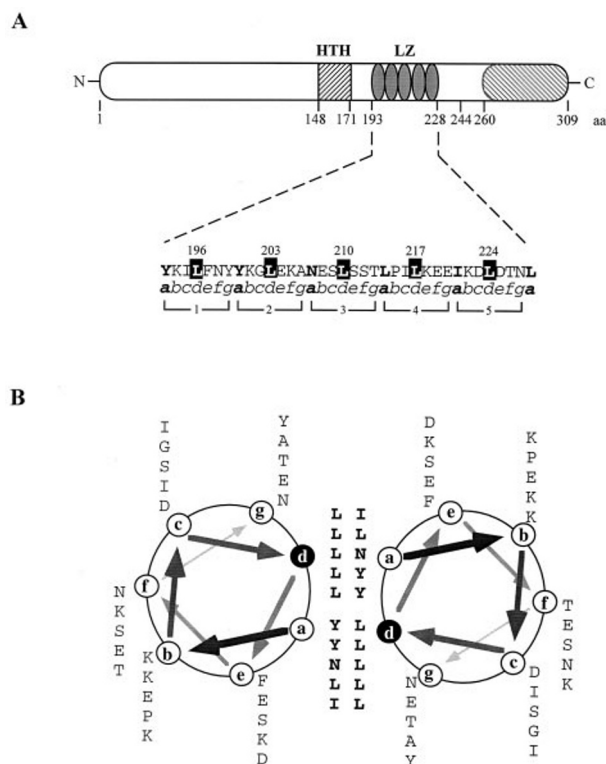


FIG. 1. Predicted domain structure of the VirB protein and disposition of the putative leucine zipper motif. A, VirB is shown at the top. The relative positions of the HTH and LZ motifs are indicated together with a predicted C-terminal trimeric coiled-coil domain (hatched). The single amino acid sequence below shows the LZ motif with the five-component heptad repeats indicated below and the leucine repeat highlighted. Repeating positions are indicated by the letters *a–g*. Residues in position *a* are in boldface type. B, a helical wheel diagram showing a head-to-head homodimer conformation to portray the predicted hydrophobic core (positions *a* and *d*). Arrows of decreasing size and intensity are directed toward the carboxyl-terminal end.

identify possible oligomerization domains in VirB. Coiled-coil domains have been described as common features allowing oligomerization of proteins (30, 31). A coiled-coil structure was predicted between positions ~190 and ~230 of VirB by the COILS program (Expasy; www.expasy.ch). In this domain, the ScanProsite program (Expasy) detected the pattern of an LZ motif commonly associated with dimerization in eukaryotic proteins such as the GCN4 yeast transcription factor protein and less frequently in prokaryotic proteins such as the IS911 transposase or antiterminator protein, BglG (32–34). The putative LZ in VirB possessed some characteristics of previously described LZ motifs (Fig. 1, A and B; Refs. 35 and 36). It consisted of 5 leucines (in position *d*) repeated every seventh residue. Residues in position *a* are also hydrophobic and, together with the leucine repeat, line up along the face of an α -helix to form a hydrophobic interface where two monomers can interact (Fig. 1B). In the central *a* position of the putative LZ, VirB contains an asparagine that is conserved in the LZ family and is thought to favor the positioning of the two coils and to help in the determination of dimerization specificity (34, 37). Residues in positions *e* and *g* normally carry opposite charges and are potentially able to form intersubunit salt bridges that stabilize the dimeric structure (31). This last characteristic was not conserved in the VirB LZ motif, suggesting that a dimeric form of this LZ motif might not be stabilized by intersubunit salt bridges. In addition, the putative LZ contains a proline residue, which is unusual in a coiled-coil structure. Finally, the C-terminal region of VirB was predicted to form a coiled-coil structure. Indeed, MULTICOIL and PARCOIL pro-

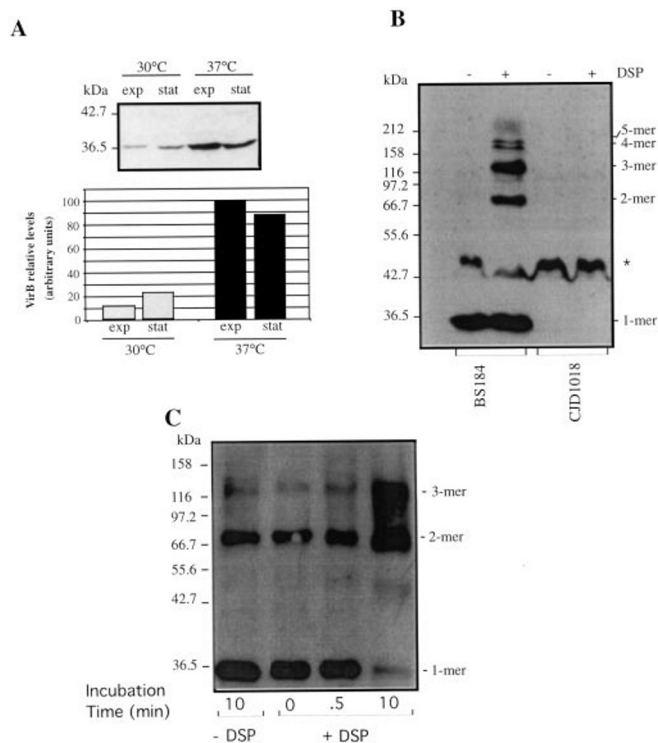
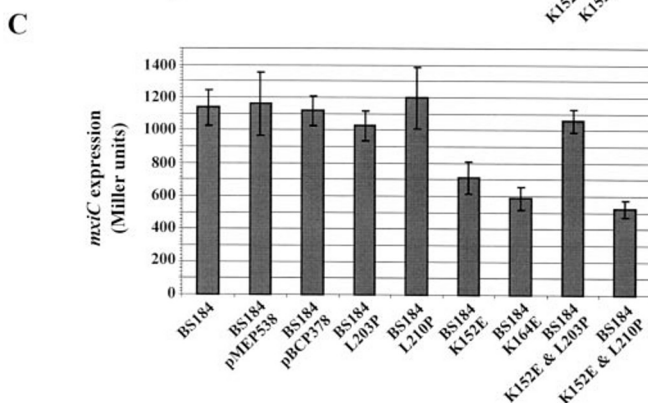


FIG. 2. *In vivo* and *in vitro* chemical cross-linking of WT VirB. A, thermal induction of VirB production. *S. flexneri* BS184 was cultured in LB-rich medium to midexponential phase or stationary phase at 30 or 37 °C. Crude protein extracts were then prepared and proteins separated through a 12% SDS-PAGE. VirB protein was visualized by immunoblotting with polyclonal anti-VirB antiserum. Below is presented a histogram representing relative levels of VirB in the different culture conditions. Levels of VirB obtained in midexponential phase at 37 °C were set to 100 for comparison. Cross-linking was performed *in vivo* (B) in growing *virB* WT bacteria (BS184) and *virB* null mutant bacteria (CJD1018) or *in vitro* (C) with purified VirB protein using DSP as described under “Experimental Procedures.” Protein bands were detected by immunoblotting with polyclonal anti-VirB antiserum. Presumed positions of VirB derivatives on the gels are indicated along the right side, together with molecular size markers along the left side. The asterisk in B indicates the position of a cross-reacting band unrelated to VirB as shown in the *virB*[−] strain CJD1018.

grams (Expasy) predicted positions ~260 to 309 of VirB to form a trimeric coiled-coil region.

VirB Can Oligomerize *In Vivo* and *In Vitro*—The presence of putative coiled-coil structures in VirB was consistent with the possibility that the protein could oligomerize. Oligomerization was evaluated *in vivo* using a cross-linking method. First, we determined the best conditions for VirB production in order to facilitate its detection. Virulence gene expression was induced in bacteria grown at 37 °C in growth media with an osmolarity similar to that of physiological saline and at a pH close to neutrality (8, 38, 39). *S. flexneri* 2a strain BS184 was cultured in the complex medium LB at 30 or 37 °C, and crude protein extracts were prepared at the midexponential or late stationary phase of growth. VirB was identified by immunodetection using a polyclonal antiserum raised against a purified N-terminal His-tagged VirB protein (Fig. 2A).² Whereas VirB was detectable at 30 °C, its production was increased by about 8-fold at 37 °C, in keeping with the well known thermoregulation of virulence gene expression in *S. flexneri*. At this temperature, VirB appeared to be somewhat more abundant in midexponential compared with late stationary growth phase. These growth conditions were then employed when performing the *in vivo* cross-linking experiments.

² C. Beloin, S. McKenna, and C. J. Dorman, unpublished data.



The putative HTH DNA-binding domain was also mutagenized. Such motifs consists of two helices that interact with the DNA. Much of this interaction is based on electrostatic interactions in which positively charged amino acids bind to the negatively charged DNA. Disruption of these interactions disrupts DNA binding (41, 42). In VirB, two positively charged lysines, Lys¹⁵² and Lys¹⁶⁴ (one in each helix), were mutated to

glutamic acids (*i.e.* negatively charged amino acids of similar size) (Fig. 3A).

We then estimated the ability of the different VirB mutants to activate structural virulence gene expression. Plasmids containing mutant VirB were transformed into a *virB*[−] background containing a *lacZ* fusion to *mxiC*, one of the structural genes subject to regulation by VirB. The production of each VirB mutant protein was confirmed by immunodetection and was comparable with WT VirB levels (data not shown). The results of β -galactosidase assays on these strains are shown in Fig. 3B. The bar graph illustrates the temperature dependence of *mxiC* expression in all of the strains, and it also reveals that multicopy wild type *virB* can only partially complement a *virB*[−] strain. This is sufficient, however, to show clear differences in expression from some of the mutants. It is clear from these data that both of the mutations in the HTH motif, K152E and K164E, reduced the ability of the protein to activate gene expression to negligible levels, thus indicating a very important role for this putative DNA-binding domain in VirB activity. This remained true for the K152E mutation when combined with a mutation in the LZ motif (K152E/L203P or K152E/L210P). However the mutants with lesions in the LZ motif showed a less clear pattern of structural gene activation. Mutation in two leucines of the LZ motif, L196E and L210H had no effect on β -galactosidase activity. However, a more severe mutation in leucine 210, L210P, like mutations L217S and L224R, reduced activity by ~50% compared with WT. Whereas, as expected, the L203V mutant was as active as the WT, the L203P substitution completely abolished activity to background levels. Therefore, mutation of four of five leucines of the LZ motif had a disruptive effect on VirB activation proficiency. This supports the prediction that the defined motif possesses structural characteristics of an LZ but also that oligomerization is required for VirB activity *in vivo*. Altering proline 215 to alanine did not appear to have an effect on VirB function. Altering asparagine 207 to a more hydrophobic or hydrophilic amino acid did not affect VirB-mediated *mxiC* activation. This suggests that this asparagine might not have the role it normally fulfills in a true LZ motif.

In order to assess whether the mutations were affecting dimer/oligomerization or some other function of the protein, the HTH mutants and the L203P/L210P mutants, which reduced or abolished structural gene expression, were co-expressed with WT VirB in a *virB*⁺ background. In this way, mutants capable of forming faulty dimers or oligomers would be expected to reduce β -galactosidase activity in the BS184 parent strain by interfering with native VirB function (*i.e.* have a *trans*-dominant phenotype). The *trans*-dominance test allowed a qualitative assessment of the ability of mutant and WT proteins to interact *in vivo*. Although the VirB derivatives with the LZ lesions were completely or partially inactive, when they were expressed in a *virB* WT background there was no negative effect on *mxiC-lacZ* expression. This suggested that the function disrupted in these mutants was oligomerization, rendering them incapable of interaction with WT VirB. On the other hand, the oligomerization of VirB was confirmed by the *trans*-dominant phenotype of HTH mutants, K152E and K164E, whose expression reduced β -galactosidase activity in BS184 by half (Fig. 3C). When the K152E mutation was combined in the same VirB polypeptide with a disruptive LZ mutation, L203P, the *trans*-dominant phenotype was relieved, confirming that the L203P mutation was disrupting the formation of faulty oligomers. The *trans*-dominant effect was retained, however, when K152E was combined in the same protein with the L210P mutation, suggesting that the L210P substitution only partially disrupted VirB oligomerization.

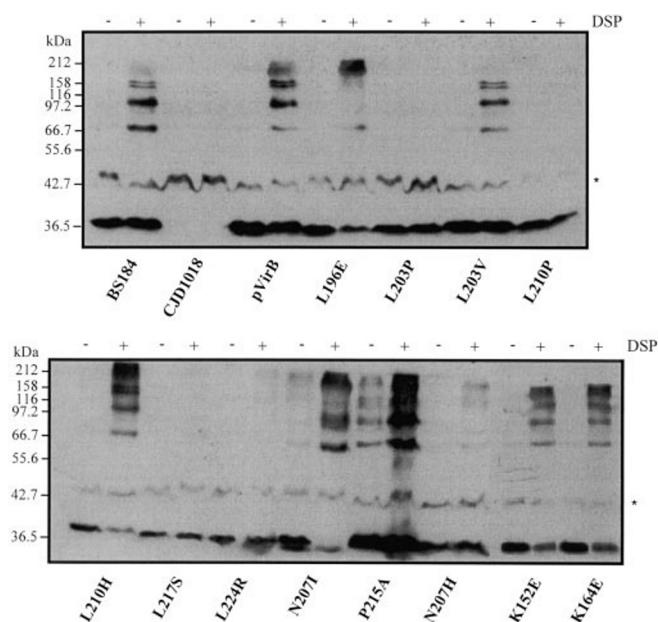
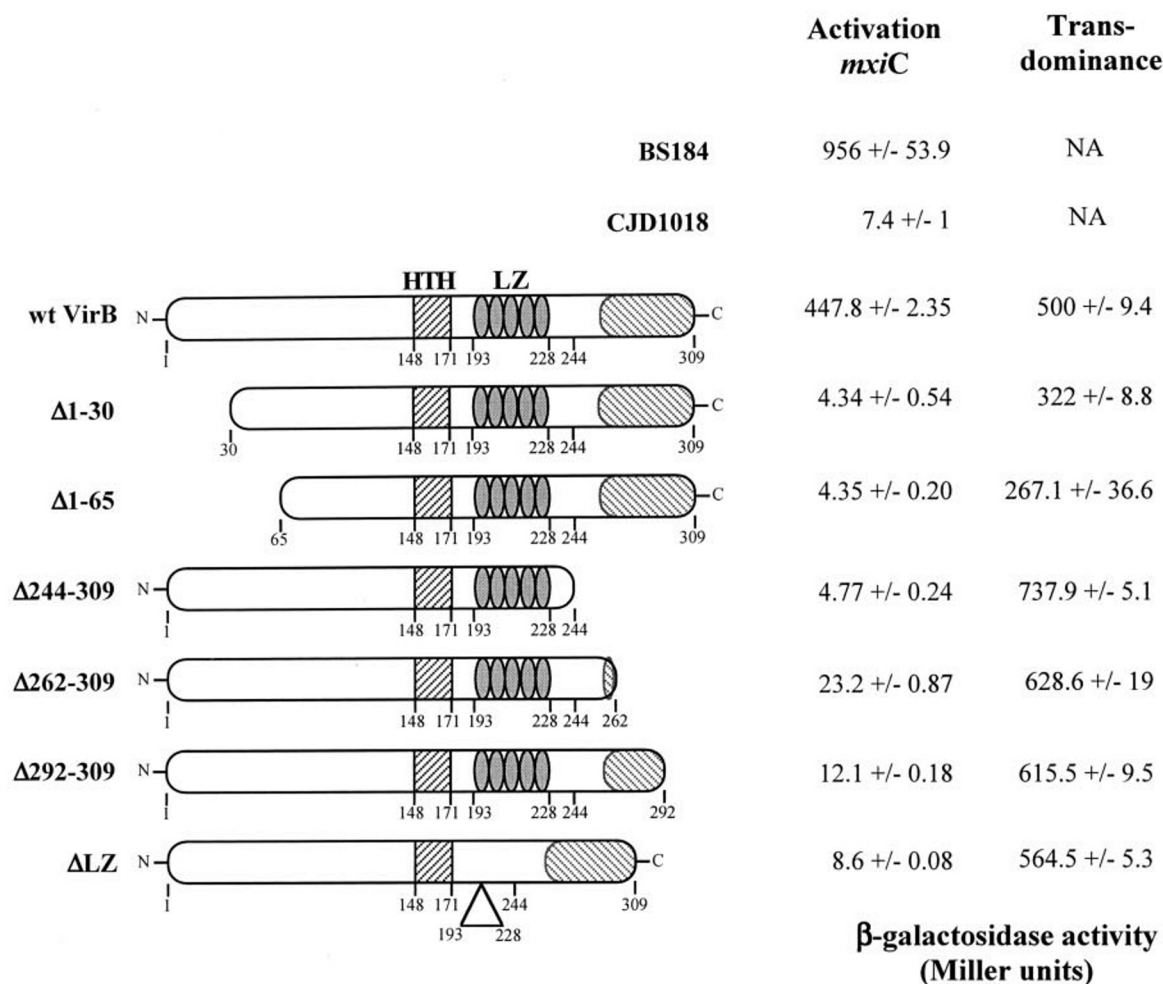


FIG. 4. *In vivo* chemical cross-linking of VirB mutants. Wild type or *virB* mutant genes were cloned in plasmid pMEP539 and transformed in a *virB*[−] strain (CJD1018). Cross-linking was performed *in vivo* in growing bacteria using DSP as described under "Experimental Procedures." Protein bands were detected by immunoblotting with polyclonal anti-VirB antiserum. Molecular size markers are indicated along the left side. The asterisk corresponds to the position of a cross-reacting band unrelated to VirB as shown in the *virB*[−] strain CJD1018.

We decided to confirm the role of the LZ motif in VirB oligomerization by *in vivo* cross-linking. Each mutant was expressed in the *virB* mutant background, and its ability to oligomerize was assessed using the DSP cross-linker (Fig. 4). Immunodetection of VirB confirmed that each mutant was expressed to a level comparable with WT level. For those amino acid substitutions that had not altered VirB activity (Fig. 3B), some oligomerization was detectable at low exposure (L196E, L203V, L210H, N207I/H, and P215A). Interestingly, P215A was able to oligomerize weakly *in vivo* in the absence of DSP, and cross-linking was stronger than WT when DSP is added. As expected, the HTH mutants, K152E, and K164E, retained WT oligomerization proficiency. On the contrary, oligomerization of those LZ mutants that had affected VirB activity *in trans* (Fig. 3B, L203P, L210P, L217S, and L224R) was not detectable at low exposure. At higher exposure, oligomerization was detectable for L210P, L217S, and L224R, whereas L203P oligomerization was still undetectable (data not shown), in agreement with the different levels of *mxiC* expression measured in these mutants. These results confirmed that the predicted LZ motif of VirB was necessary for oligomerization *in vivo* and that the level of oligomerization also determined the levels of VirB activity *in vivo*.

VirB Possesses Another Multimerization Domain—We demonstrated the importance of VirB oligomerization for VirB activity *in vivo* and showed that a LZ motif was necessary for this oligomerization. However, LZ motifs normally promote strict dimerization of proteins rather than formation of higher oligomers. Analysis of putative structural domains of VirB revealed the presence, in the last ~50 amino acids, of a coiled-coil domain predicted to form a triple coil structure (Fig. 1A). Therefore, we decided to study the role of this domain in VirB activity. N-terminal and C-terminal VirB truncates were constructed, and their *mxiC* activation abilities, *trans*-dominance phenotypes (Fig. 5A), and oligomerization proficiencies were assessed (Fig. 5B). Despite being able to oligomerize normally, two N-terminal truncates (Δ 1–30 and Δ 1–65) were unable to

A



B

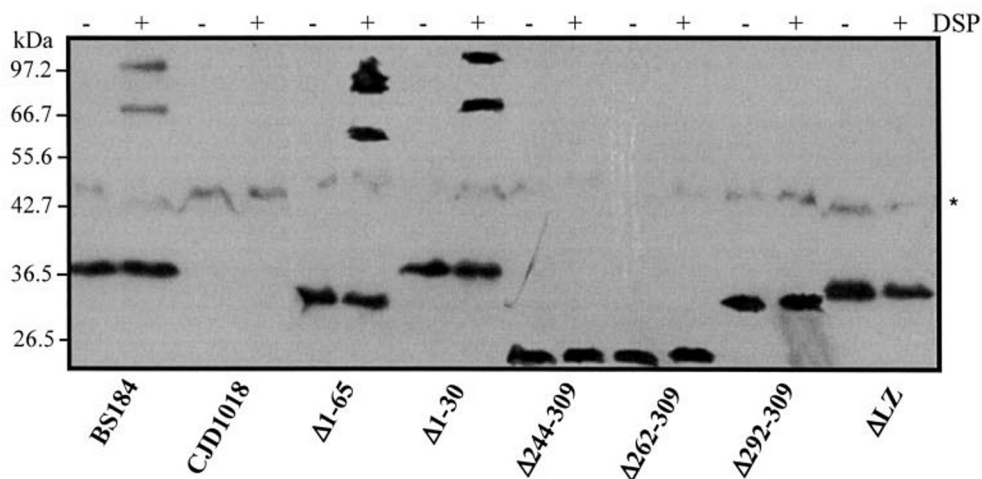

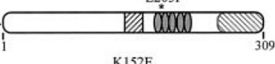
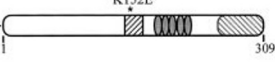
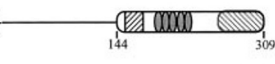
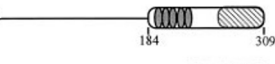
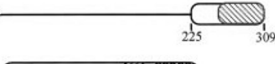

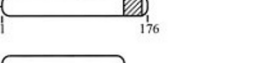

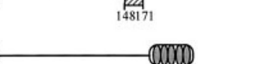
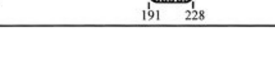


FIG. 5. Construction of VirB truncates and effect on virulence cascade activation *in vivo*. A, the different VirB truncates constructed are presented with the relevant putative structural domains. They were expressed on pMEP539 plasmid, transformed in the *virB*⁻ strain CJD1018. *mxiC* activation ability of each VirB truncate was estimated at 37 °C by measuring the β-galactosidase activity of the *mxiC-lacZ* fusion. *mxiC* activity observed in the *virB*⁺ strain, BS184, and the *virB*⁻ strain, CJD1018, are also presented for comparison. *Trans*-dominance was estimated by expressing each truncate in a *virB*⁺ background (strain BS184), and resulting *mxiC* expression was measured at 37 °C. S.D. values are indicated. NA, not applicable. B, oligomerization ability of VirB truncates was assessed by *in vivo* DSP cross-linking as described earlier (Fig. 4). Molecular size markers are indicated along the left side. The asterisk corresponds to the position of a cross-reacting band unrelated to VirB.

FIG. 6. *In vivo* protein oligomerization assay. Proteins that were tested in this assay included wild type (*wt*) and the N-terminal DNA-binding domain of λ cI repressor, chimeric proteins composed of the DNA-binding domain of cI and leucine zipper domain of GCN4, wild type, or mutant VirB. Oligomerization proficiency of these domains was assessed by their ability to functionally replace the natural C-terminal domain of the λ cI repressor conferring biological activity to the N-terminal DNA-binding domain of the same repressor (*i.e.* immunity to phage λ). Failure to oligomerize the N-terminal domain of λ cI repressor results in sensitivity to phage λ . *a*, superinfection immunity (*Imm.*) indicates that there were no plaques formed after infection, whereas the number of plaques was always greater at 20 plaques/ml for superinfection sensitivity (*Sens.*). *b*, the constructs were also introduced in strain JH372, containing a phage λ where the *lacZ* gene is fused to the lytic promoter P_{O_L} . Their oligomerization proficiency was assessed by measuring β -galactosidase activity. The data expressed in Miller units represent an average of three independent experiments. S.D. values were <10% in each case.

Plasmid	Protein	Superinfection immunity ^a	β -galactosidase activity (Miller units) ^b
-	-	Sens.	8673
pZ150	Vector backbone	Sens.	8404
pFG157	cI (wt)	Imm.	304
pKH101	cI (1-115)	Sens.	3065
pJH370	cI (1-115)-GCN4 LZ	Imm.	86
pSM-VirB	cI (1-115)- 	Imm.	220
pSM-L203P	cI (1-115)- 	Sens.	1533
pSM-K152E	cI (1-115)- 	Imm.	270
pSM-Δ1-144	cI (1-115)- 	Imm.	164
pSM-Δ1-184	cI (1-115)- 	Imm.	168
pSM-Δ1-225	cI (1-115)- 	Imm.	355
pSM-Δ232-309	cI (1-115)- 	Sens.	2381
pSM-Δ176-309	cI (1-115)- 	Sens.	1015
pSM-Δ147-309	cI (1-115)- 	Sens.	1884
pSM-HTH	cI (1-115)- 	Imm.	214
pSM-LZ	cI (1-115)- 	Sens.	2654

activate *mxiC* expression and possessed a *trans*-dominant phenotype when co-expressed with WT VirB. This suggested that while the N-terminal region of VirB might include an activation domain and/or a DNA-binding domain, it was not required for oligomerization.

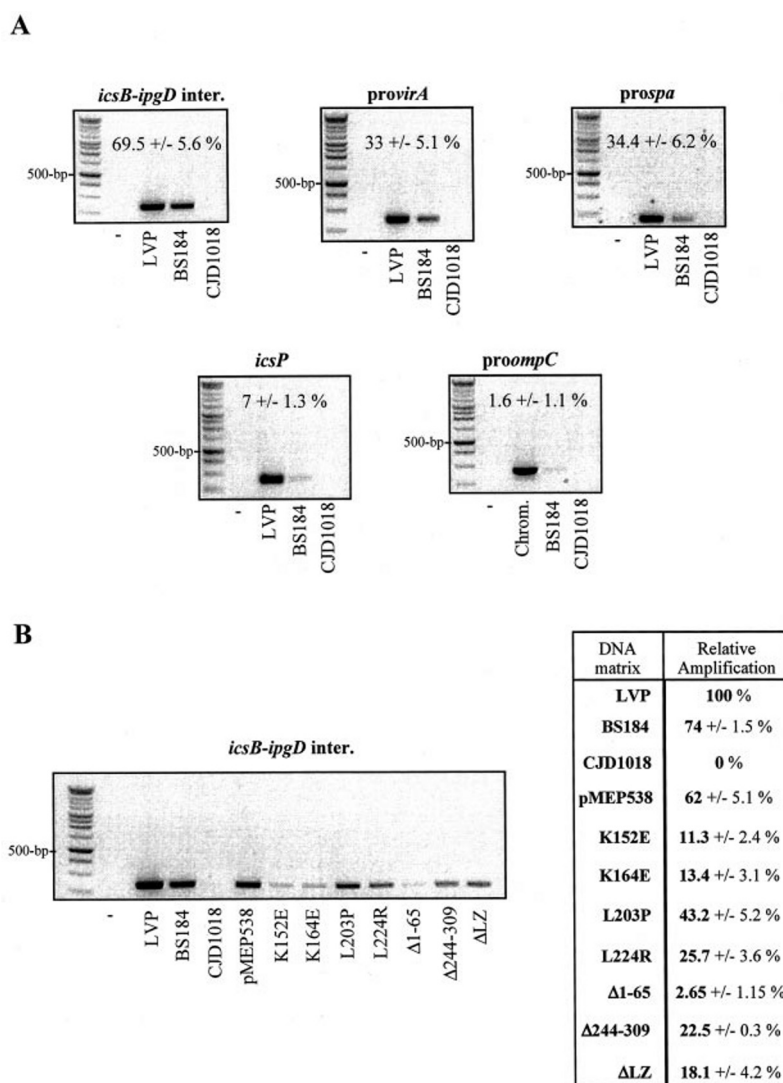
At the C terminus, the removal of only the last 17 amino acids of the triple coil domain (Δ 292–309) had the same effect on VirB activity as a complete removal of this domain (Δ 244–309 and Δ 262–309). These VirB truncates were completely deficient in *mxiC* activation and importantly had no *trans*-dominant phenotype (Fig. 5A). Strikingly, these two last truncates migrated at the same position despite an 18-amino acid difference in size. This may be due to a conformational change in one of the truncates or to degradation of the larger truncate. These data indicated that the C-terminal domain of VirB was probably necessary for oligomerization to occur. DSP cross-links experiments confirmed this hypothesis; VirB C-terminal truncates could not oligomerize (Fig. 5B).

As expected from previous results, deletion of the LZ motif led to a loss of *mxiC* activation, did not create a *trans*-dominant phenotype (Fig. 5A) and suppressed VirB oligomerization (Fig. 5B), thus confirming that the LZ motif was also necessary for oligomerization. VirB oligomerization is thus promoted by two domains, the LZ motif and the last ~65 amino acids of the C terminus. Each domain was necessary, but each was individually insufficient to promote oligomerization.

An *In Vivo* Assay to Assess Oligomerization Proficiency of the VirB Domains—An *in vivo* oligomerization assay was used to confirm definitely the role of the C terminus and of the LZ motif in multimerization. The test relied on the ability of the putative

oligomerization domain of the protein of interest to replace functionally the natural oligomerization domain in the C terminus of the phage λ cI repressor, thereby conferring biological activity on the N-terminal DNA-binding domain of the same repressor, *i.e.* immunity to phage λ (43). Eleven different cI-VirB fusion proteins were constructed (Fig. 6). After verifying that each chimeric protein was expressed (data not shown), these constructs were assayed for their ability to oligomerize in two different systems. The first involved a phage sensitivity test in which the chimeric proteins were expressed in a λ -sensitive strain, which was then infected with cI null mutant phage. The second involved the expression of the constructs in a strain containing a *lacZ* fusion to the λ lytic promoter P_{O_L} , where oligomerization was measured by the repression of β -galactosidase expression. Whereas the N-terminal DNA-binding domain of cI-(1–115) (pKH101) was unable to confer immunity to phage λ , WT cI (pFG157) and chimeric cI-(1–115)-GCN4 LZ (pJH370) were clearly active in repressing the P_{O_L} lytic promoter (Fig. 6). Like the GCN4 LZ, the full-length VirB (pSM-VirB) and the K152E VirB mutant (pSM-K152E), each conferred biological activity on the N-terminal DNA-binding domain of cI, allowing repression of the P_{O_L} promoter. The L203P mutation (pSM-L203P) restored phage sensitivity, confirming that the LZ motif of VirB was necessary for dimerization and also that the C-terminal region did not promote oligomerization in the absence of an intact LZ motif. As expected, a deletion of the last 77 amino acids of VirB (pSM- Δ 232–309) restored phage sensitivity, confirming that this region contains a domain that is necessary for oligomerization and that the LZ motif did not promote dimerization in absence of an intact C-terminal domain.

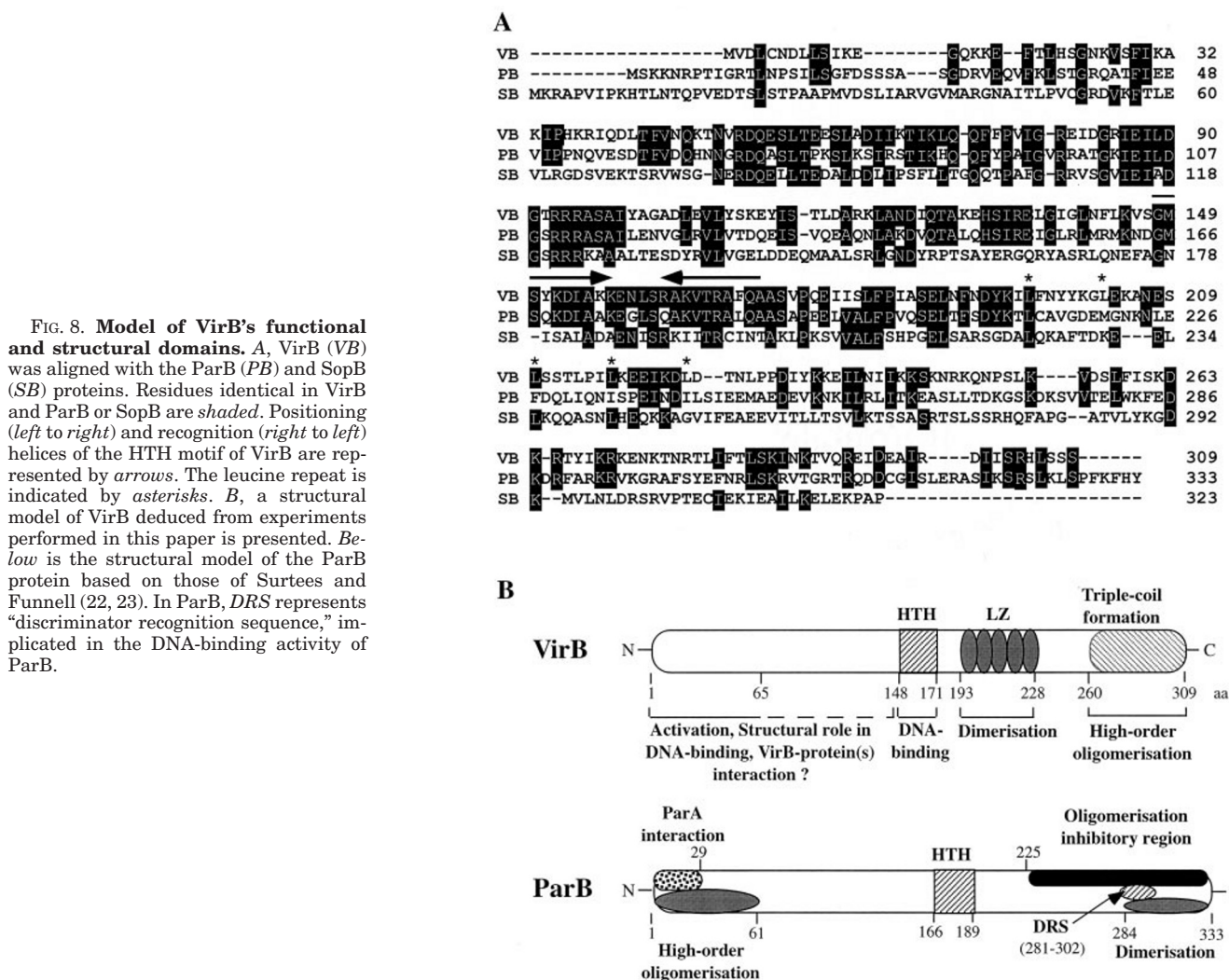
FIG. 7. *In vivo* association of WT VirB and VirB mutants/truncates identified through cross-linked DNA immunoprecipitation. A, polyclonal absorbed antibodies were used to immunoprecipitate VirB from cell extracts after formaldehyde cross-linking *in vivo* (see "Experimental Procedures"). After reversal of the cross-links, DNA in the immunoprecipitate was amplified by PCR using six sets of primer pairs from four different promoter regions localized on the LVP of *S. flexneri* (*icsB-igpD* intergenic region, *virA*, *spa*, and promoter regions), one internal gene region on the LVP (*icsP* gene), and one promoter region of a chromosomal gene (*ompC* promoter region). -, no DNA in the PCR; LVP, PCR with purified large virulence plasmid DNA; BS184, DNA from the immunoprecipitate from wild type cells; CJD1018, DNA from the immunoprecipitate from a *virB* null mutant. Each gel correspond to a representative result of at least three independent experiments. Percentages *inset* in each gel represent relative quantified PCR amplification levels obtained from DNA of the WT immunoprecipitate (BS184) compared with those obtained from DNA of the purified LVP. Those percentages correspond to PCR quantification performed on at least three independent experiments. S.D. values are indicated. B, representative VirB mutants were expressed in the *virB*⁻ strain CJD1018, and the *in vivo* cross-link DNA immunoprecipitation experiment was repeated as in A. The DNA immunoprecipitated was amplified by PCR using a primer set for *icsB-igpD* intergenic region. The gel presented corresponds to a representative result of three independent experiments. A table is presented with relative levels of PCR amplification calculated for each DNA immunoprecipitated compared with LVP purified DNA (average of three independent experiments).



Surprisingly, this C-terminal domain alone (pSM-Δ1-225) could partially repress the P_r promoter sufficiently to confer immunity to phage λ , showing that this isolated domain could promote oligomerization of VirB to some extent. This oligomerization became stronger when the LZ motif was added to the C-terminal VirB domain (pSM-Δ1-144 and pSM-Δ1-184). The isolated VirB LZ motif was unable to promote repression of the P_r promoter (pSM-LZ), showing that this motif alone was also not sufficient to promote normal oligomerization. As expected, the N-terminal region of VirB was not able to promote oligomerization, since the 144-309 (pSM-Δ1-144) and 184-309 (pSM-Δ1-184) regions of VirB conferred immunity to phage λ , whereas region 1-147 (pSM-Δ147-309) could not restore repression by λ . Remarkably, in the absence of the two characterized VirB oligomerization motifs, the HTH motif could also promote oligomerization of the N-terminal domain of λ (pSM-HTH). This may be due to an unusual conformation adopted by the motif in the absence of the rest of the protein.

VirB Binds Directly to Promoter Regions of Structural Virulence Genes *In Vivo*—Previous attempts at bandshift experiments using purified VirB or cell lysates were unable to demonstrate specific binding of VirB to the promoters of the *S. flexneri* structural virulence genes (20).² *In vitro*, VirB bound DNA but with no particular specificity, and a reconstituted system in *E. coli* where VirB was expressed *in trans* from an inducible promoter failed to show direct activation by VirB of virulence gene promoter fusions to *lacZ* (20).² We

suspected, however, that *in vivo* in *S. flexneri*, the situation might be different and that VirB was in fact a direct activator of the structural virulence genes. To test this hypothesis, we employed a technique derived from a chromatin immunoprecipitation assay recently used with success in prokaryotes to identify DNA-binding proteins targets (44, 45) (see "Experimental Procedures"). Formaldehyde was added *in vivo* to *S. flexneri* cells during exponential growth at 37 °C to cross-link protein and DNA. Cells were lysed, and the DNA was sheared by sonication. The VirB-DNA complexes were immunoprecipitated using specific VirB polyclonal antibodies, the cross-links were reversed by heating, and the precipitated DNA was analyzed by PCR. Six sets of primers were used in the PCR assay to test for the presence of four promoter regions from structural virulence genes/operons suspected to be directly activated by VirB (*icsB-igpD* intergenic region, *virA* and *spa* promoter regions) and also for the presence of two negative control DNAs. These were an internal fragment of the *icsP* gene of *S. flexneri* coding for a plasmid-encoded IcsA-cleaving protease and the promoter region of the chromosomal *ompC* gene. DNA from the four structural virulence gene promoters was clearly immunoprecipitated, whereas only trace amounts of DNA were detected for the negative controls (Fig. 7). In parallel experiments, no DNA was detected from a *virB* null mutant (CJD1018). These results strongly suggest that *in vivo* VirB specifically binds to the promoters of these structural virulence genes. This binding



could reflect a direct interaction of VirB with the DNA of these regions or perhaps co-binding with another protein or regulatory factor.

The same chromatin immunoprecipitation assay-based technique was used to analyze the interaction of representative VirB mutants/truncates with the *icsB-igpD* intergenic region. We observed comparable quantities of immunoprecipitated DNA for WT VirB expressed from *virB* in its native location (BS184) or on a multicopy plasmid (pMEP538). In strains expressing either HTH mutant, the levels of DNA immunoprecipitated were considerably reduced (Fig. 7). This indicated not only that this HTH motif acts *in vivo* as a functional DNA-binding domain but also that VirB binding to the promoter of structural virulence genes was occurring through direct interaction between VirB and DNA. The levels of DNA immunoprecipitated in mutants where VirB oligomerization ability was affected (LZ mutants and C-terminal and LZ truncates) were also reduced, albeit not to the same extent as with the HTH mutants. Such mutations may have affected DNA binding indirectly by modifying the global VirB structure. It was also possible that VirB bound DNA more efficiently when able to oligomerize. Interestingly, levels of DNA immunoprecipitated from a strain expressing an N-terminal truncate of VirB were drastically reduced ($\Delta 1-65$). Since the same truncate was able to oligomerize normally (Fig. 5B), it is unlikely that the effect observed in this chromatin immunoprecipitation assay experiment was due to disruption of the VirB secondary structure.

This suggests that the N-terminal domain of VirB is necessary for efficient binding of VirB to DNA.

DISCUSSION

Hitherto, the role of the VirB protein in the positive control of virulence gene expression in *S. flexneri* has been implied only from genetic studies (10, 15, 46, 47). The amino acid sequence of VirB reveals a protein with strong similarities to plasmid partition proteins such as ParB from phage P1 and SopB from plasmid F (17) rather than one belonging to any known family of transcription factors (Fig. 8). Immunological analysis of VirB expression as a function of growth phase and temperature shows that its intracellular concentration increases markedly when the culture is shifted to 37 °C, the temperature at which virulence gene expression is maximal, and VirB levels are higher in cells in the exponential rather than in the stationary phase of growth (Fig. 2A). The protein is still detectable at 30 °C in both exponential and stationary phase cultures. Under these conditions, virulence gene expression is repressed but is also still detectable (Figs. 2 and 3). Thus, there is a clear correlation between the intracellular concentration of VirB and the expression of the virulence structural genes. This is supported by the observation that when increasing levels of VirB were produced artificially at 30 °C, the expression of the virulence structural genes increased proportionally to VirB quantity (data not shown).

In silico analysis of the predicted secondary structure of VirB

reveals two motifs found in transcription factors. These are a central HTH followed by a putative LZ (Fig. 8). The HTH motif is also found in ParB, but the LZ feature is poorly conserved. However, the portion of ParB that includes these features has been shown to be involved in protein-protein interactions (23). In this investigation, these features of VirB were studied by mutagenesis to establish whether or not they made contributions to its biological function.

The VirB LZ motif is unusual in lacking residues required to produce a salt bridge to stabilize dimers and in containing a proline residue likely to destabilize the helical structure. Also, the central asparagine residue does not appear to have the function normally associated with this residue in LZ motifs. Work with anti-VirB antibody shows that VirB can form oligomers, with structures up to pentamers being detected in the presence of the DSP cross-linking agent *in vivo* (Fig. 2B). This is in contrast to the simple dimers normally associated with LZ interactions, suggesting the presence in VirB of extra oligomerization domains. Disruption of the LZ motif by amino acid substitutions establishes a key role for this component of VirB in virulence gene activation. In particular, converting Leu²⁰³ to Pro abolished the ability of the protein to activate an *mxlC-lacZ* fusion (Fig. 3). This substitution also prevented VirB from oligomerizing (Fig. 4). Similar effects on oligomerization are seen with substitutions of the leucines at positions 210, 217, and 224 (Fig. 3). Consistent with these findings, a complete deletion of the LZ also abolishes oligomerization (Fig. 5). Loss of the LZ prevents VirB from activating gene expression (Fig. 5) and reduces notably its ability to bind to DNA (Fig. 7). The LZ cannot promote protein-protein interactions in isolation. When this component of VirB is fused to the DNA-binding domain of λ cI repressor, no oligomerization is detected. The C terminus of VirB contains a second oligomerization domain, and deletions here prevent VirB oligomerization, even when the LZ is present (Fig. 5). Thus, the LZ motif is unable to promote oligomerization without the C terminus. Unlike the LZ motif, the C-terminal domain promotes some oligomerization when fused to the DNA-binding domain of the cI repressor (Fig. 6), although VirB mutants lacking the C terminus are no better than LZ deletion mutants at binding to DNA (Fig. 7). However, in the full length VirB protein without an intact LZ, no oligomers of any size can be detected, although the C terminus is present (Figs. 4 and 5). It appears therefore that not only may initial interactions occur through the LZ but also that the dimers formed by the LZ motif are stable only in the presence of this C-terminal domain. The formation of C-terminal coiled-coil structures may compensate for the relatively unstable dimers promoted by LZ-LZ interactions that lack inter-salt bridges and may also promote the formation of higher ordered VirB oligomers. Clearly, the LZ motif of VirB has several features that distinguish it from more conventional leucine zippers. Nevertheless, it is essential to the biological function of the VirB protein. It is reasonable to conclude that full function in VirB requires both oligomerization of LZ and C-terminal domains whose activities are mutually dependent, a situation described previously for some eukaryotic proteins and for the bacterial protein BglG (32). However, it should be noted that among eukaryotic proteins, the presence of additional oligomerization domains is not necessarily indicative of an inability to form salt bridges at LZ motifs (30).

The presence of the proline within the LZ motif is highly unusual, and we are not aware of other examples of such an occurrence. Interestingly, the P215A derivative was found to form multimers more easily than the WT protein, doing so *in vivo* in the absence of cross-linking agent (Fig. 4). Perhaps the

removal of the proline enhanced the abilities of the LZ motifs to interact, thus promoting formation of stable oligomers.

Reversing the charges of key residues in either helix of the HTH motif abolishes the ability of VirB to activate virulence gene expression (Fig. 3). These mutants are *trans*-dominant, as one might expect for proteins with lesions that alter DNA binding without interfering with oligomerization. Neither mutant retains DNA binding activity (Fig. 7), and cross-linker treatment confirms that the HTH mutants still oligomerize (Fig. 4). Interestingly, the isolated HTH motif is able to confer oligomerization activity on the DNA-binding domain of the cI repressor (Fig. 6). This may reflect a previously described ability of HTH sequences to promote the formation of protein fibrils when expressed out of context (48, 49). Certainly, there is little evidence that the HTH contributes significantly to VirB oligomerization (Fig. 4).

This work has shown that VirB is a DNA-binding protein that interacts specifically *in vivo* with the promoters of the virulence genes it is known to regulate (Fig. 7). It has not been established that this interaction is effected by VirB alone, and it remains a possibility that VirB requires a co-factor for specific binding. We have found previously that purified VirB can bind DNA nonspecifically *in vitro*. The protein appears to oligomerize on the DNA, forming complexes that are retained in the wells in electrophoretic mobility shift assays.² *In vivo*, the protein interacts specifically with its target promoters. This may indicate that VirB operates *in vivo* with a co-factor, possibly a protein, to ensure specificity. Inspection of the nucleotide sequences of the target promoters reveals no obvious regions of homology that might indicate a binding site consensus sequence. It is possible that the preferred binding site is marked by a structural feature, such as a region of intrinsic DNA curvature. A comparison may be made with ParB, which has a partner protein called ParA. Interaction with ParA occurs via the N terminus of ParB, a region that is strongly homologous to the N terminus of VirB (see Refs. 21 and 50; Fig. 8). In the case of VirB, the N terminus makes no contribution to protein oligomerization (Fig. 6); its deletion results in no loss of oligomerization activity (Fig. 5), but loss of the N terminus strongly affects VirB binding activity at DNA sequences normally bound by this protein (Fig. 7). Thus, it is possible that the N terminus of VirB is required for interaction with a co-factor involved in directing VirB to DNA, by analogy with ParA and ParB. A search for this putative co-factor will be a future goal of research on VirB function.

We demonstrated a direct correlation between VirB intracellular concentration and VirB oligomerization proficiency with the expression of the virulence structural genes (Figs. 2, 3, and 5) and also that VirB binds *in vivo* to the promoters of those structural virulence genes (Fig. 7). Therefore, VirB oligomerization on DNA may be an important part of the activation mechanism of those genes, and this could involve exclusion of a repressor from the promoters activated by VirB. Elucidating this mechanism will also constitute a future goal of our investigation of VirB function.

Acknowledgments—We thank Jim Hu, Liat Fux, and Orna Amster-Choder for the *in vivo* protein oligomerization detection system. For helpful and stimulating discussions, we thank the present and past members of the Dorman laboratory (especially Megan E. Porter) and Maria Mavris, Claude Parsot, and the other members of the TMR Network on Regulation of Gene Expression in Bacterial Pathogenesis.

REFERENCES

1. Sansonetti, P. J. (1999) *Am. Soc. Microbiol. News* **65**, 611–617
2. High, N., Mounier, J., Prévost, M. C., and Sansonetti, P. J. (1992) *EMBO J.* **11**, 1991–1999
3. Ménard, R., Sansonetti, P. J., and Parsot, C. (1996) *EMBO J.* **13**, 5293–5302
4. Wassef, J., Karen, D. F., and Mailloux, J. L. (1989) *Infect. Immun.* **57**, 858–863
5. Dorman, C. J., and Porter, M. E. (1998) *Mol. Microbiol.* **29**, 677–684

6. Blocker, A., Gounon, P., Larquet, E., Niebuhr, K., Cabiaux, V., Parsot, C., and Sansonetti, P. J. (1999) *J. Cell Biol.* **147**, 683–696
7. Maurelli, A. T., Baudry, B., d'Hauteville, H., Hale, T. L., and Sansonetti, P. J. (1985) *Infect. Immun.* **49**, 164–171
8. Porter, M. E., and Dorman, C. J. (1994) *J. Bacteriol.* **176**, 4187–4191
9. Porter, M. E., and Dorman, C. J. (1997) *J. Bacteriol.* **179**, 6537–6550
10. Tobe, T., Yoshikawa, M., Mizuno, T., and Sasakawa, C. (1993) *J. Bacteriol.* **175**, 6142–6149
11. Dorman, C. J., McKenna, S., and Beloin, C. (2001) *Int. J. Med. Microbiol.* **290**, 89–96
12. Falconi, M., Colonna, B., Prosseda, G., Micheli, G., and Gualerzi, C. O. (1998) *EMBO J.* **17**, 7033–7043
13. Nakayama, S. I., and Watanabe, H. (1998) *J. Bacteriol.* **180**, 3522–3528
14. Porter, M. E., and Dorman, C. J. (2002) *J. Bacteriol.* **184**, 531–539
15. Tobe, T., Yoshikawa, M., and Sasakawa, C. (1995) *J. Bacteriol.* **177**, 1094–1097
16. Day, W. A. J., and Maurelli, A. T. (2001) *Infect. Immun.* **69**, 15–23
17. Watanabe, H., Arakawa, E., Ito, K. I., Kato, J. I., and Nakamura, A. (1990) *J. Bacteriol.* **172**, 619–629
18. Abeles, A. L., Friedman, S. A., and Austin, S. J. (1985) *J. Mol. Biol.* **185**, 261–272
19. Bignell, C., and Thomas, C. M. (2001) *J. Biotechnol.* **91**, 1–34
20. Porter, M. E. (1998) *The Regulation of Virulence Gene Expression in Shigella flexneri*, Ph.D. thesis, Trinity College, Dublin
21. Radnedge, L., Davis, M. A., and Austin, S. A. (1996) *EMBO J.* **15**, 1155–1162
22. Surtees, J. A., and Funnell, B. E. (2001) *J. Biol. Chem.* **276**, 12385–12394
23. Surtees, J. A., and Funnell, B. E. (1999) *J. Bacteriol.* **181**, 5898–5908
24. Dodd, I. B., and Egan, B. J. (1990) *Nucleic Acids Res.* **18**, 5019–5026
25. Miller, J. H. (1972) *Experiments in Molecular Genetics* (Press, C. S. H., ed) Cold Spring Harbor, NY
26. Hays, L. B., Chen, Y. S., and Hu, J. C. (2000) *BioTechniques* **29**, 288–290
27. Orlando, V. (2000) *Trends Biochem. Sci.* **25**, 99–104
28. Strahl-Bolsinger, S., Hecht, A., Luo, K., and Grunstein, M. (1997) *Genes Dev.* **11**, 83–93
29. Brennan, R. G., and Matthews, B. W. (1989) *J. Biol. Chem.* **264**, 1903–1906
30. Baxevanis, A. D., and Vinson, C. R. (1993) *Curr. Opin. Genet. Dev.* **3**, 278–285
31. Lupas, A. (1996) *Trends Biochem. Sci.* **21**, 375–382
32. Boss, A., Nussbaum-Shochat, A., and Amster-Choder, O. (1999) *J. Bacteriol.* **181**, 1755–1766
33. Haren, L., Polard, P., Ton-Hoang, B., and Chandler, M. (1998) *J. Mol. Biol.* **283**, 29–41
34. O'Shea, E. K., Klemm, J. D., Kim, P. S., and Alber, T. (1991) *Science* **254**, 539–544
35. Alber, T. (1992) *Cur. Opin. Gen. Dev.* **2**, 205–210
36. Landschulz, W. H., Johnson, P. F., and McKnight, S. L. (1988) *Science* **240**, 1759–1764
37. Gonzalez, L. J., Woolfson, D. N., and Alber, T. (1996) *Nat. Struct. Biol.* **3**, 1011–1018
38. Hromockyj, A. E., and Maurelli, A. T. (1989) *Infect. Immun.* **57**, 2963–2970
39. Maurelli, A. T., Blackmon, B., and Curtis, R., III (1984) *Infect. Immun.* **1984**, 195–201
40. Hu, J. C., O'Shea, E. K., Kim, P. S., and Sauer, R. T. (1990) *Science* **250**, 1400–1403
41. Harrison, S. C. (1991) *Nature* **353**, 715–719
42. Ochs, M., Angerer, A., Enz, S., and Braun, V. (1996) *Mol. Gen. Genet.* **250**, 455–465
43. Zeng, X., and Hu, J. C. (1997) *Gene (Amst.)* **185**, 245–249
44. Lin, D. C.-H., and Grossman, A. D. (1998) *Cell* **92**, 675–685
45. Rodionov, O., Lobocka, M., and Yarmolinsky, M. (1999) *Science* **283**, 546–549
46. Adler, B., Sasakawa, C., Tobe, T., Makino, S., Komatsu, K., and Yoshikawa, M. (1989) *Mol. Microbiol.* **3**, 627–635
47. Tobe, T., Nagai, S., Okada, N., Adler, B., Yoshikawa, M., and Sasakawa, C. (1991) *Mol. Microbiol.* **5**, 887–893
48. Fezoui, Y., Hartley, D. M., Walsh, D. M., Selkoe, D. J., Osterhout, J. J., and Teplow, D. B. (2000) *Nat. Struct. Biol.* **7**, 1095–1099
49. Jiang, J., de Hertog, J., and Hunter, T. (2000) *Mol. Cell. Biol.* **20**, 5917–5929
50. Bouet, J.-Y., Surtees, J. A., and Funnell, B. E. (2000) *J. Biol. Chem.* **275**, 8213–8219
51. Hanahan, D. (1983) *J. Mol. Biol.* **166**, 557–580
52. Studier, F. W., and Meffel, B. W. (1986) *J. Mol. Biol.* **189**, 113–130
53. Veletrop, J. S., Dijkhuizen, M. A., van't Hof, R., and Postma, P. W. (1995) *Gene (Amst.)* **153**, 63–65
54. Zagursky, R. J., and Berman, M. L. (1984) *Gene (Amst.)* **27**, 183–191
55. Pouwels, P. H. (1985) *Cloning Vectors*, pp. 451–460, North-Holland, Amsterdam